Stretched two-nucleon configurations in ^{210}Pb

P. von Neumann-Cosel,[1] P. Schenk,[2] U. Fister,[2,*] T. K. Trelle,[2,*] and R. Jahn[2]
[1]*Institut für Kernphysik, Technische Hochschule Darmstadt, DW-6100 Darmstadt, Federal Republic of Germany*
[2]*Institut für Strahlen- und Kernphysik, Universität Bonn, DW-5300 Bonn, Federal Republic of Germany*
(Received 28 August 1992)

The ^{208}Pb(α,^{2}He)^{210}Pb reaction has been investigated at about 55 MeV incident energy. The angular distributions of prominent transitions were analyzed with the distorted-wave Born approximation. At low excitation energies, states built on $2g_{9/2}$ single-particle strength are found, while at higher energies configurations including $1j_{15/2}$ strength dominate. Together with the predictions of the crude shell model the main configurations of most observed transitions were identified. The results are compared to shell-model calculations with the Kuo-Herling residual interaction modified by Warburton and Brown.

PACS number(s): 21.10.Hw, 21.60.Cs, 25.55.Hp, 27.80.+w

I. INTRODUCTION

The spectroscopy of nuclei with two particles or holes relative to a closed-shell nucleus has always played a major role in the determination of two-body matrix elements and as a crucial test of residual interactions [1,2]. Experimental information on these nuclei is further needed as benchmarks of larger shell-model calculations.

Here, new data on ^{210}Pb are presented, a nucleus with two neutrons with respect to the doubly magic ^{208}Pb. Experimental studies of ^{210}Pb are rather scarce [3], mainly because of the missing availability of suitable targets. So far, studies of the two-neutron (nn) transfer reaction (t,p), of inelastic scattering, and of the (^{7}Li,αn) reaction have been reported [4–7].

We have investigated the nn transfer reaction ^{208}Pb(α,^{2}He)^{210}Pb which might be regarded as a counterpart of (t,p). While the former preferentially populates low-spin states and has been extensively used to study the role of pairing in the ground-state (g.s.) wave function, the latter is known [8] to selectively excite stretched configurations, i.e., two-neutron states coupled to maximum spin. This feature is related to the large negative Q values, respectively large angular momentum mismatches, of α induced two-neutron transfer reactions. For an incident energy of about 55 MeV an optimum angular momentum transfer of $(11-15)\hbar$ is estimated for a surface reaction.

The (α,^{2}He) reaction has been utilized for systematic studies of stretched nn states in the p, sd, and fp shells [9–11]. With semiconductor detector telescopes as used in the present experiment extension to heavier nuclei becomes increasingly difficult because of the strong yield of elastic scattering under forward angles, which are important to distinguish between different angular momentum transfer values. A first attempt to investigate ^{210}Pb with the (α,^{2}He) reaction has been reported by van Driel *et al.* [12], but they failed to resolve individual states.

*Present address: AEG, DW-7900 Ulm, Germany.

II. EXPERIMENT

The experiment was performed with a 55-MeV ^{4}He beam from the Bonn Isochronous Cyclotron. A self-supporting ^{208}Pb target of 675 μg/cm^2, isotopically enriches to 97%, and a 200-μg/cm^2 natural carbon target were used. The thicknesses were determined by normalizing the elastic-scattering cross sections to optical model calculations at forward angles (see Sec. III). In order to determine absolute cross sections, the total charge for each run was collected in a Faraday cup.

The unbound reaction product ^{2}He was detected by measuring the two breakup protons in coincidence. The detector consisted of a double ΔE-E telescope with large area position-sensitive 300-μm Si ΔE counters and 5-mm Si(Li) E counters. The setup which takes advantage of the kinematic focusing induced by the pp final-state interaction is described in detail in Ref. [11]. Elastic α scattering was simultaneously measured with the telescope described in Ref. [13].

Beam intensities ranged from 30 to 300 nA, limited by the electronic dead time of the ^{2}He detection system. Typical acquisition times for one detector position were 20–50 h. The (α,^{2}He) reaction was measured at four angles between 24° and 50° in order to kinematically identify states and extract angular distributions. By setting electronic gates, the position information was utilized to gain three angular distribution points for each detector position. The method of extraction of differential cross sections in the center-of-mass system and further details of the data analysis are explained in Ref. [11].

A particular problem of this experiment was the presence of carbon carried with the beam and deposited on the target during the experiment. This led to effective carbon target thicknesses for the ^{12}C(α,^{2}He)^{14}C contamination reaction which were large enough to cover a substantial part of the ^{210}Pb strength in the spectra. Therefore, the ^{14}C spectra were measured with the identical detector setting and subtracted after normalization to the well-known [8] dominant transitions of the ^{12}C(α,^{2}He)^{14}C reaction.

III. DISTORTED-WAVE BORN APPROXIMATION ANALYSIS

The angular distributions obtained for the ^{208}Pb(α,^{2}He)^{210}Pb reaction were analyzed in the framework of the zero-range distorted-wave Born approximation (DWBA) using the computer code DWUCK4 [14]. A direct stripping process from the incident α particle was assumed where the neutron pair is transferred in a relative S state (spin $S=0$ and isospin $T=1$).

Optical model parameters were extracted from an analysis of the simultaneously measured elastic α scattering. The computer code PTOLEMY [15] was used for the parameter search. Two sets of parameters were used as starting values, viz. those of Refs. [11] and [16]. The resulting best-fit parameters are given in Table I. Figure 1 displays the experimental and calculated elastic-scattering cross sections divided by the Rutherford cross section as a function of the center-of-mass angle. The quality of description is quite similar for both sets. Preference has been given to the model parameter set with the shallower real part based on Ref. [16], since it provided overall slightly better results for the transfer calculations. Also, the real part of this potential is adjusted to the volume integral value extracted from a resolution of the discrete ambiguity at high energies [17].

The averaged mass-, charge-, and energy-dependent deuteron potential of Hinterberger *et al.* [18] was used for the exit channel. However, an increase of the real potential depth was found necessary stemming from the smaller effective scattering energy due to the double charge of a ^{2}He with respect to a deuteron. As discussed in Ref. [11] the strongly oscillating $L=0$ g.s. angular distribution provides a sensitive test of this correction. Accordingly, the real potential depth has been varied to give the best reproduction of the ^{208}Pb(α,^{2}He)^{210}Pb(g.s.) transition (see Fig. 3).

Furthermore, it is open whether a volume or surface absorption term should be used. While a surface imaginary term is favored by elastic-scattering data [19,20] and has, e.g., been used for a study of the ^{208}Pb(α,d)^{210}Bi reaction [16] at slightly lower energies, there is also empirical evidence that volume absorption sometimes provides the better description of angular distributions [11,13,21,22] for α-induced two-nucleon transfer reactions. We have tested both approaches and found slightly better results for the g.s. as well as excited states with a surface imaginary term. We note, however, that the shape differences are small, particularly for large L values, and the preference is solely based on the empirical findings.

Details of the form factor calculation are described in Ref. [11]. The variations resulting from alternate methods of calculation have been discussed in Refs. [13,23] and are generally small.

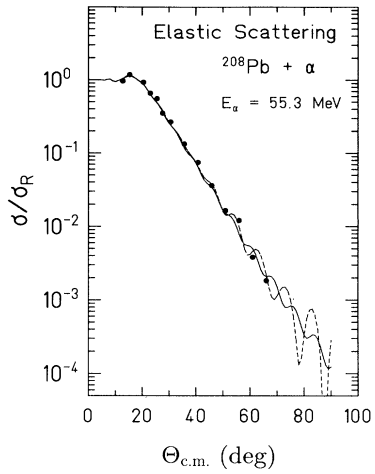

FIG. 1. Angular distributions of elastic α scattering on ^{208}Pb. The dashed and solid lines are optical model fits with the parameter sets 1 and 2 of Table I, respectively.

IV. RESULTS AND DISCUSSION

A spectrum of the ^{208}Pb(α,^{2}He)^{210}Pb reaction at $\Theta_{lab}=24°$ is presented in Fig. 2. A total of nine states could be unambiguously identified from kinematics with a typical energy resolution of 200–250 keV. Two of them, at 2.52 and 3.99 MeV, show an enlarged linewidth which indicates doublets. In Fig. 2 the subtracted carbon spectrum has been scaled to leave a small rest which enables one to locate the position of strong ^{12}C(α,^{2}He)^{14}C states. One should keep in mind that for larger angles the ^{14}C levels are shifted to lower E_{lab} values relative to ^{210}Pb levels which restricts the problem to the g.s. contribution.

Angular distributions of the differential cross sections of the identified states are presented in Fig. 3. The absolute values are estimated to be correct within 30%, with the main error source from relatively poor statistics. The subtraction of the carbon spectra induces an additional uncertainty of approximately ±10%. The solid and dashed lines correspond to DWBA calculations for the indicated L transfer values.

Since the forward angle region, which is most sensitive to distinguish between different L values, is not accessible in the present experiment because of the very strong elastic-scattering rate on a high Z target, the quality of the data is not sufficient for stringent L assignments. However, in many cases low L values can be ruled out or

TABLE I. Optical model potential parameters for the entrance (target + α) channel used in the DWBA analysis.

V (MeV)	r_v (fm)	a_v (fm)	W (MeV)	r_w (fm)	a_w (fm)	r_c (fm)	Reference
225.2	1.26	0.64	16.2	1.41	0.99	1.3	[11]
169.0	1.26	0.72	37.8	1.34	0.90	1.3	[16]

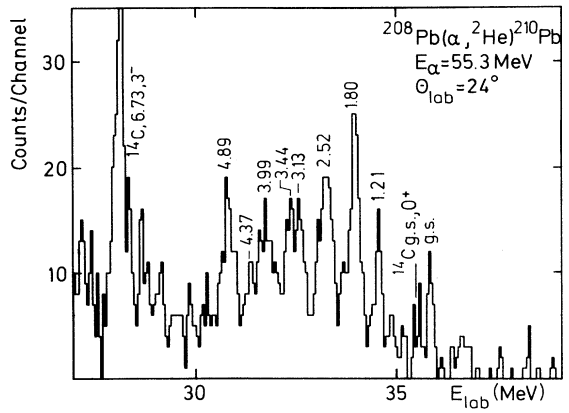

FIG. 2. Spectrum of the ^{208}Pb(α,^{2}He)^{210}Pb reaction at $E_\alpha = 55.2$ MeV and $\Theta_{lab} = 24°$.

possible angular momenta can be limited. Additionally, the particular sensitivity of the (α,^{2}He) reaction to excite stretched configurations permits easy comparison with simple shell-model predictions of the corresponding excitation energies.

The crude shell model (CSM) of Chan *et al.* [24] provides a simple mean to calculate the energies of stretched two-nucleon states and was found to successfully describe them in *sd*- and *fp*-shell nuclei [11,25,26] with a typical deviation of ±500 keV from the experimental values. Starting from the independent particle ansatz, the binding energy of a two-neutron state $(j_1 j_2)_J$ in a final nucleus $A+2$ can be written as

$$B(A+2,(j_1j_2)_J) = B(A+1,j_1) + B(A+1,j_2) + \langle j_1 j_2 | V_{res} | j_1, j_2 \rangle_J \ . \quad (1)$$

Here, $B(A+1,j_{1,2})$ denote the binding energies of the corresponding single-particle states and $\langle\ \rangle$ stands for the residual interaction matrix element coupled to total spin J. Conversion to excitation energies leads to

$$E_x(A+2,(j_1j_2)_J) = E_x(A+1,j_1) + E_x(A+1,j_2) + \langle j_1 j_2 | V_{res} | j_1, j_2 \rangle_J + E_{pair} \quad (2)$$

with E_{pair} describing the pairing energy of the valence neutrons in the $A+2$ nucleus. It can be calculated from the g.s. binding energies of the nuclei A, $A+1$ and $A+2$,

$$E_{pair}(nn) = B(A,\text{g.s.}) + B(A+2,\text{g.s.}) - 2B(A+1,\text{g.s.}) \ . \quad (3)$$

The systematics of two-body matrix elements (TBME) [1,2] show that the interaction is generally small for stretched configurations of like nucleons ($T=1$). The CSM simply takes

$$\langle j_1 j_2 | V_{res} | j_1 j_2 \rangle = 0 \quad (4)$$

and calculates the excitation energies of two-neutron configurations from Eq. (2) with this assumption. Since the basis of this approach, excitation of pure configurations, is particularly well fulfilled in the present case, the typical accuracy of the CSM should be much better than the above-quoted error.

Figure 4 displays the CSM predictions together with the experimental energies of the observed ^{210}Pb levels. For many states, this comparison provides strong hints on dominant transitions as indicated by the dashed lines. The DWBA calculations for a particular level are restricted to those CSM configurations which deviate no more than ±200 keV. The DWBA results are summarized in Table II, where the assumed configurations and

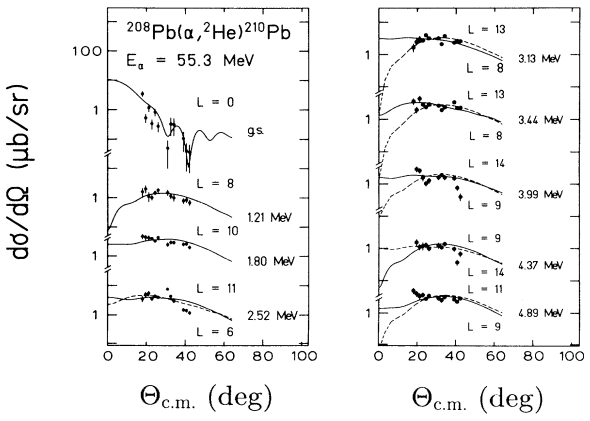

FIG. 3. Angular distributions of ^{210}Pb states populated in the reaction ^{208}Pb(α,^{2}He)^{210}Pb. The solid and dashed lines are DWBA calculations. For a particular state the L transfer value shown above the curves always corresponds to the solid line and the value below corresponds to the dashed line.

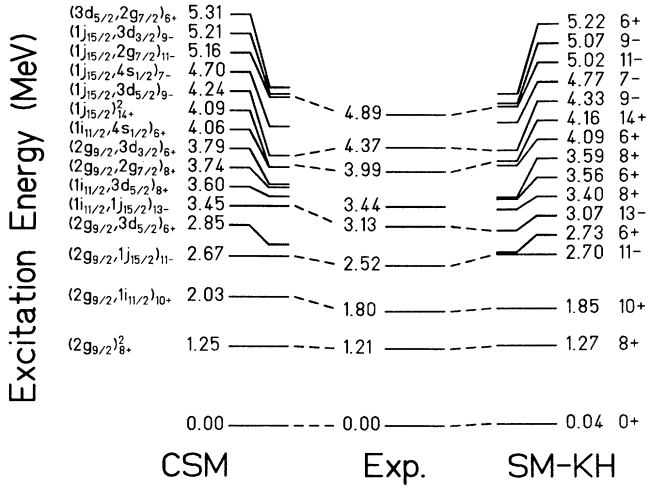

FIG. 4. Left part (CSM): Energy spectrum predicted by the crude shell model [24] and assumed two-particle configurations. Middle part (Exp.): Experimental energy spectrum observed in the ^{208}Pb(α,^{2}He)^{210}Pb reaction. Right part (SM-KH): Shell-model energy spectrum calculated from the modified Kuo-Herling residual interaction [29]. The dashed lines indicate favored configuration assignments.

the normalization factors are given in columns 3 and 4. Nonstretched configurations are not considered, since the resulting cross sections are typically at least an order of magnitude smaller than for the stretched states.

As described in Sec. III, the g.s. angular distribution has been used to fix the real potential depth correction for the exit channel with respect to the values of Ref. [18]. The 1.21-MeV state is known from earlier work as the 8^+ member of the $(2g_{9/2})^2$ ground-state multiplet. An $L=8$ calculation describes the data reasonably and the resulting normalization constant compares well with other deduced values. The 1.80-MeV transition was tentatively assigned $J^\pi=10^+$ by Flynn *et al.* [4]. The present values fully confirm the assignment of a pure $(2g_{9/2},1i_{11/2})_{10^+}$ configuration.

The most likely candidates for the 2.52-MeV state are $(2g_{9/2},1j_{15/2})_{11^-}$ and $(2g_{9/2},3d_{5/2})_{6^+}$. The data slightly favor an $L=11$ angular distribution, but the scattering of the experimental data is large. The DWBA results indicate that the 2.52-MeV level might well be an unresolved doublet of both configurations. The 3.13-MeV angular distribution is well explained, both in magnitude and in shape, assuming a $(1i_{11/2},1j_{15/2})_{13^-}$ transition. Also, the CSM predicts no other state nearby. For the 3.44-MeV level, various $L=6$ and 8 transitions are considered. The corresponding angular distributions are hard to distinguish in the angular region experimentally accessed. The normalization constants also permit no clear distinction. Furthermore, due to the small energy difference considerable mixing of the $(2g_{9/2},2g_{7/2})_{8^+}$ and $(1i_{11/2},3d_{5/2})_{8^+}$ configurations must be expected as discussed below.

The $(1j_{15/2})^2_{14^+}$ and $(1j_{15/2},3d_{5/2})_{9^-}$ configurations are prime candidates for the 3.99- and 4.37-MeV transitions. Again, we are not able to distinguish from the angular distributions. A tentative assignment of $J^\pi=14^+$ to the 3.99-MeV state is given following the CSM prediction. Additional strength in the 3.99-MeV doublet might come from the $(2g_{9/2},3d_{3/2})_{6^+}$ and $(2g_{9/2},2g_{7/2})_{8^+}$ configurations which would explain the too large $(1j_{15/2})^2_{14^+}$ normalization. For the 4.89-MeV state, a $(1j_{15/2},2g_{7/2})_{11^-}$ transition is favored both from shape and strength compared to a $(1j_{15/2},3d_{3/2})_{9^-}$ transition.

Assuming an inert ^{208}Pb core, full shell-model calculations can be performed. An effective realistic residual interaction has been derived by Kuo and Herling [27] from the Hamada-Johnston potential [28] by reaction matrix techniques. This interaction has recently been thoroughly tested and optimized by Warburton and Brown [29]. This set of matrix elements has been used for a calculation of ^{210}Pb.

The resulting level scheme (restricted to dominantly stretched states) is displayed in the right part of Fig. 4. The scheme generally agrees well with the CSM results and essentially confirms most suggested assignments discussed above. In detail some differences from the CSM can be observed. The energies of the $(2g_{9/2},1i_{11/2})_{10^+}$ and $(1i_{11/2},1j_{15/2})_{13^-}$ configurations correspond much better to the experimental values. The differences are due to the large attractive TBME of these configurations.

TABLE II. DWBA calculations for prominent transitions of the ^{208}Pb$(\alpha,^2$He$)^{210}$Pb reaction using the pure configurations suggested by the CSM and shell-model wave functions.

E_x (MeV)	J^π	*nn* configuration	N	Shell-model wave function[a]	N
g.s.	0^+	$(2g_{9/2})^2$	225±140	$0.82(2g_{9/2})^2+0.42(1i_{11/2})^2-0.31(1j_{15/2})^2+0.13(3d_{5/2})^2$ $+0.06(4s_{1/2})^2+0.17(2g_{7/2})^2+0.13(3d_{3/2})^2$	120±75
				$0.78(2g_{9/2})^2+0.42(1i_{11/2})^2-0.34(1j_{15/2})^2+0.19(3d_{5/2})^2$ $+0.09(4s_{1/2})^2+0.16(2g_{7/2})^2+0.12(3d_{3/2})^2$	100±65[b]
1.21	8^+	$(2g_{9/2})^2$	36±12		
1.80	10^+	$(2g_{9/2},1i_{11/2})$	30±9		
2.52	11^-	$(2g_{9/2},1j_{15/2})$	46±21		
	6^+	$(2g_{9/2},3d_{5/2})$	77±33	$0.78(2g_{9/2},3d_{5/2})+0.56(1i_{11/2})^2+0.19(2g_{9/2},3d_{3/2})$	68±30
3.13	13^-	$(1i_{11/2},1j_{15/2})$	28±7		
3.44	8^+	$(2g_{9/2},2g_{7/2})$	24±10	$0.77(2g_{9/2},2g_{7/2})-0.19(1i_{11/2})^2-0.58(1i_{11/2},3d_{5/2})+0.11(2g_{9/2},1i_{11/2})$	20±8
		$(1i_{11/2},3d_{5/2})$	72±30	$0.80(1i_{11/2},3d_{5/2})+0.59(2g_{9/2},2g_{7/2})$	1200±360
	6^+	$(2g_{9/2},3d_{3/2})$	37±11	$0.60(2g_{9/2},3d_{3/2})-0.18(2g_{9/2},3d_{5/2})+0.42(2g_{9/2},2g_{7/2})-0.14(1i_{11/2})^2$ $-0.56(1i_{11/2},3d_{5/2})-0.23(1i_{11/2},4s_{1/2})-0.14(1j_{15/2})^2-0.12(3d_{5/2},2g_{7/2})$	235±60
		$(1i_{11/2},4s_{1/2})$	290±80	$0.94(1i_{11/2},4s_{1/2})-0.30(1i_{11/2},3d_{5/2})$	265±75
3.99	14^+	$(1j_{15/2})^2$	120±60		
	9^-	$(1j_{15/2},3d_{5/2})$	61±48	$0.99(1j_{15/2},3d_{5/2})-0.13(1j_{15/2},3d_{3/2})$	105±80
4.37	9^-	$(1j_{15/2},3d_{5/2})$	29±12	$0.99(1j_{15/2},3d_{5/2})-0.13(1j_{15/2},3d_{3/2})$	50±20
	14^+	$(1j_{15/2})^2$	59±15		
4.89	11^-	$(1j_{15/2},2g_{7/2})$	26±10		
	9^-	$(2g_{9/2},3d_{3/2})$	56±31	$0.74(1j_{15/2},3d_{3/2})+0.14(1j_{15/2},3d_{5/2})+0.66(1j_{15/2},2g_{7/2})$	165±90
	6^+	$(3d_{5/2},3g_{7/2})$	67±12	$0.98(3d_{5/2},2g_{7/2})+0.10(2g_{9/2},3d_{3/2})$	57±10

[a]Residual interaction of Ref. [29]. Except for the g.s. only amplitudes >0.1 are shown.
[b]Pairing model wave function from Ref. [30].

The $(1j_{15/2})^2_{14^+}$ state is shifted somewhat higher, between the experimental values of 3.99 and 4.37 MeV. However, the $(1j_{15/2},3d_{5/2})_{9^-}$ level is shifted also, which leaves the above conclusions on these two states unchanged.

In general, all the shifts with respect to the CSM result from the inclusion of the TBME rather than mixing between the states. The wave functions of the states considered here show little mixing, at least for $J \geq 10$. The $(2g_{9/2},2g_{7/2})_{8^+}$ and $(1i_{11/2},3d_{5/2})_{8^+}$ configurations mix strongly due to their nearly degenerate unperturbed energies. Also, configuration mixing is important for the 6^+ and to some extent for the 9^- states. In the rightmost columns of Table II shell-model wave functions and the resulting normalization constants in the DWBA analysis are given. In cases of significant mixing, the normalization constants usually become larger if nonstretched configurations are admixed. Thus, $(1j_{15/2},3d_{3/2})_{9^-}$ can be largely excluded for the 4.89-MeV state. For the same reason, prominent excitation of 6^+ states is unlikely.

The g.s. transition is apparently much better described with a realistic wave function than assuming a pure $(2g_{9/2})^2_{0^+}$ configuration. A comparison to the pairing model [30] reveals a very similar g.s. structure with the main difference being a somewhat larger $(2g_{9/2})^2$ amplitude at the expense of higher-lying $(3d_{5/2})^2$ and $(4s_{1/2})^2$ strength. The normalization is large with respect to high L transfer values, but this deficiency is most likely due to a not ideal optical model parametrization for the poorly matched $L=0$ transition.

If one omits the g.s. transition an average normalization constant $N \simeq 30$ is obtained with only small deviations. Due to the somewhat different choice of optical model parameters, this result cannot be directly compared to the survey of the *fp* shell [11]. We note that using parameters in line with the approach of Ref. [11] comparable normalization constants would be obtained, but the overall description deteriorates as discussed in Sec. III.

V. CONCLUSIONS

A study of the ^{208}Pb$(\alpha,^2$He$)^{210}$Pb reaction was performed and new information on stretched two-nucleon configurations was obtained. The DWBA description of the angular distributions together with the CSM predictions served as a guide for likely configuration assignments. A comparison with full shell-model calculations based on the effective, realistic Kuo-Herling interaction showed that configuration mixing plays some role for $J=6-9$ states, but does not affect higher J states. A DWBA normalization constant $N \simeq 30$ is obtained with little scattering for the assigned shell-model wave functions.

The present results indicate that the experimentally observed transitions are essentially pure two-nucleon states, i.e., ^{208}Pb core excitations are of no importance. Because of the simple structure these states might be used as benchmarks in model descriptions of the ^{208}Pb mass region. In particular, the excitation energies of the high J configurations are a direct test of the involved two-body matrix elements.

ACKNOWLEDGMENTS

We would like to thank the technical staff of the Bonn Isochronous Cyclotron for their assistance in the experiment and H. Hodde for preparation of the targets. We are indebted to E. K. Warburton for providing us with a set of the Kuo-Herling matrix elements. This work was supported by the Bundesministerium für Forschung und Technologie of the Federal Republic of Germany.

[1] J. P. Schiffer and W. W. True, Rev. Mod. Phys. **48**, 191 (1976).
[2] W. W. Daehnick, Phys. Rep. **96**, 319 (1983).
[3] E. Browne, Nucl. Data Sheets **65**, 209 (1992); B. Harmatz, *ibid.* **34**, 735 (1981).
[4] E. R. Flynn, G. J. Igo, R. A. Broglia, S. Landowne, V. Paar, and B. Nilsson, Nucl. Phys. A **195**, 97 (1972).
[5] D. J. Decman, J. A. Becker, J. B. Carlson, R. G. Lanier, L. G. Mann, G. L. Struble, K. H. Maier, W. Stöffl, and R. K. Sheline, Phys. Rev. C **28**, 1060 (1983).
[6] C. Ellegaard, P. D. Barnes, E. R. Flynn, and J. Igo, Nucl. Phys. A **162**, 1 (1971).
[7] T. P. Sjoreen, U. Gerg, and D. B. Fossan, Phys. Rev. C **21**, 1838 (1980).
[8] R. Jahn, G. J. Wozniak, D. P. Stahel, and J. Cerny, Phys. Rev. Lett. **37**, 812 (1976).
[9] R. Jahn, D. P. Stahel, G. J. Wozniak, R. J. de Meijer, and J. Cerny, Phys. Rev. C **18**, 9 (1978).
[10] R. Jahn, U. Wienands, D. Wenzel, and P. von Neumann-Cosel, Phys. Lett. B **150**, 331 (1985).
[11] U. Fister, R. Jahn, P. von Neumann-Cosel, P. Schenk, T. K. Trelle, D. Wenzel, and U. Wienands, Phys. Rev. C **42**, 2375 (1990).
[12] J. van Driel, R. Kamermans, and R. J. de Meijer, Nucl. Phys. A **350**, 109 (1980).
[13] D. Wenzel, R. Jahn, P. von Neumann-Cosel, and U. Wienands (submitted to Nucl. Phys. A).
[14] P. D. Kunz, program DWUCK4 (unpublished).
[15] M. H. McFarlane and S. C. Pieper, program PTOLEMY, Argonne National Laboratory Report No. ANL 76-11, 1976.
[16] W. W. Daehnick, M. J. Spisak, and J. R. Comfort, Phys. Rev. C **23**, 1906 (1981).
[17] G. R. Satchler, *Direct Nuclear Reactions* (Oxford University, New York, 1983).
[18] F. Hinterberger, G. Mairle, H. Schmidt-Rohr, G. J. Wagner, and P. Turek, Nucl. Phys. A **111**, 265 (1968).
[19] G. Mairle, K. T. Knöpfle, H. Riedesel, G. J. Wagner, V. Bechtold, and L. Friedrich, Nucl. Phys. A **339**, 61 (1980).
[20] W. W. Daehnick, J. D. Childs, and R. Vrcelj, Phys. Rev. C **21**, 2233 (1980).
[21] Y. Kadota, K. Ogino, K. Obari, Y. Taniguchy, T. Tanabe, M. Yasue, and J. Schmizu, Nucl. Phys. A **458**, 523 (1986).
[22] U. Fister, T. K. Trelle, D. Wenzel, R. Jahn, P. von Neumann-Cosel, and P. Schenk (submitted to Nucl. Phys. A).

[23] A. van der Woude and R. J. de Meijer, Nucl. Phys. A **258**, 199 (1976).
[24] T. U. Chan, M. Agard, J. F. Bruandet, and C. Morand, Phys. Rev. C **19**, 244 (1979).
[25] T. U. Chan, Phys. Rev. C **36**, 838 (1987).
[26] P. von Neumann-Cosel, U. Fister, R. Jahn, P. Schenk, T. K. Trelle, D. Wenzel, and U. Wienands (submitted to Nucl. Phys. A).
[27] T. T. S. Kuo and G. Herling, U.S. Naval Research Laboratory Report No. 2258, 1971; G. H. Herling and T. T. S. Kuo, Nucl. Phys. A **181**, 283 (1972).
[28] T. Hamada and I. D. Johnston, Nucl. Phys. **34**, 382 (1962).
[29] E. K. Warburton and B. A. Brown, Phys. Rev. C **43**, 602 (1991).
[30] L. Ferreira, R. Liotta, C. H. Dasso, R. A. Broglia, and A. Winther, Nucl. Phys. A **426**, 276 (1984).